

1 **Identification of lower-order inositol phosphates (IP<sub>5</sub> and IP<sub>4</sub>)**  
2 **in soil extracts as determined by hypobromite oxidation and**  
3 **solution <sup>31</sup>P NMR spectroscopy**

4 Jolanda E. Reusser<sup>1</sup>, René Verel<sup>2</sup>, Daniel Zindel<sup>2</sup>, Emmanuel Frossard<sup>1</sup> and Timothy I.  
5 McLaren<sup>1</sup>

6 <sup>1</sup>Department of Environmental Systems Science, ETH Zurich, Lindau, 8325, Switzerland

7 <sup>2</sup>Department of Chemistry and Applied Biosciences, ETH Zurich, Zurich, 8093, Switzerland

8 *Correspondence to:* Jolanda E. Reusser (jolanda.reusser@usys.ethz.ch)

9 **Abstract.** Inositol phosphates (IP) are a major pool of identifiable organic phosphorus (P) in soil. However, insight  
10 on their distribution and cycling in soil remains limited, particularly of lower-order IP (IP<sub>5</sub> and IP<sub>4</sub>). This is because  
11 the quantification of lower-order IP typically requires a series of chemical extractions, including hypobromite  
12 oxidation to isolate IP, followed by chromatographic separation. Here, for the first time, we identify the chemical  
13 nature of organic P in four soil extracts following hypobromite oxidation using solution <sup>31</sup>P NMR spectroscopy  
14 and transverse relaxation (T<sub>2</sub>) experiments. Soil samples analysed include A horizons from a Ferralsol (Colombia),  
15 a Cambisol and a Gleysol from Switzerland, and a Cambisol from Germany. Solution <sup>31</sup>P NMR spectra of the  
16 phosphomonoester region on soil extracts following hypobromite oxidation revealed an increase in the number of  
17 sharp signals (up to 70), and an on average 2-fold decrease in the concentration of the broad signal compared to  
18 the untreated soil extracts. We identified the presence of four stereoisomers of IP<sub>6</sub>, four stereoisomers of IP<sub>5</sub>, and  
19 scyllo-IP<sub>4</sub>. We also identified for the first time two isomers of *myo*-IP<sub>5</sub> in soil extracts: *myo*-(1,2,4,5,6)-IP<sub>5</sub> and  
20 *myo*-(1,3,4,5,6)-IP<sub>5</sub>. Concentrations of total IP ranged from 1.4 to 159.3 mg P/kg<sub>soil</sub> across all soils, of which  
21 between 9 % and 50 % were comprised of lower-order IP. Furthermore, we found that the T<sub>2</sub> times, which are  
22 considered to be inversely related to the tumbling of a molecule in solution and hence its molecular size, were  
23 significantly shorter for the underlying broad signal compared to the sharp signals (IP<sub>6</sub>) in soil extracts following  
24 hypobromite oxidation. In summary, we demonstrate the presence of a plethora of organic P compounds in soil  
25 extracts, largely attributed to IP of various order, and provide new insight on the chemical stability of complex  
26 forms of organic P associated with soil organic matter.

27

28    1       **Introduction**

29    Inositol phosphates (IP) are found widely in nature and are important for cellular function in living organisms.  
30    They are found in eukaryotic cells where they operate in ion-regulation processes, as signalling or P storage  
31    compounds (Irvine and Schell, 2001). The basic structure of IP consists of a carbon ring (cyclohexanehexol) with  
32    one to six phosphorylated centers (IP<sub>1-6</sub>) and up to nine stereoisomers (Angyal, 1963; Cosgrove and Irving, 1980).  
33    An important IP found in nature is *myo*-IP<sub>6</sub>, which is used as a P storage compound in plant seeds. Another  
34    important species of IP is that of *myo*-(1,3,4,5,6)-IP<sub>5</sub>, which is present in most eukaryotic cells at concentrations  
35    ranging from 15 to 50  $\mu$ M (Riley et al., 2006). Species of IP<sub>1-3</sub> are present in phospholipids such as  
36    phosphatidylinositol diphosphates and are an essential structural component of the cell membrane system  
37    (Strickland, 1973; Cosgrove and Irving, 1980).

38    Inositol phosphates have been reported to comprise more than 50 % of total organic phosphorus (P<sub>org</sub>) in some  
39    soils (Cosgrove and Irving, 1980; McDowell and Stewart, 2006; Turner, 2007). Four stereoisomers of IP have  
40    been detected in soils, with the *myo* stereoisomer being the most abundant (56 %), followed by *scyllo* (33 %), *neo*  
41    and D-*chiro* (11 %) (Cosgrove and Irving, 1980; Turner et al., 2012). The largest input of *myo*-IP<sub>6</sub> to the soil occurs  
42    via the addition of plant seeds (Turner et al., 2002). However, the addition of *myo*-IP<sub>6</sub> to soil can also occur via  
43    manure input because monogastric animals are mostly incapable of digesting *myo*-IP<sub>6</sub> without the addition of  
44    phytases to their diets (Leytem et al., 2004; Leytem and Maguire, 2007; Turner et al., 2007b). An exception to this  
45    are pigs, which were found to at least partially digest phytate (Leytem et al., 2004), and transgenic pigs expressing  
46    salivary phytase (Golovan et al., 2001; Zhang et al., 2018). The accumulation of *myo*-IP<sub>6</sub> in soil occurs due to the  
47    negative charge of the deprotonated phosphate groups, which can coordinate to the charged surfaces of Fe- and  
48    Al-(hydro)-oxides (Anderson et al., 1974; Ognalaga et al., 1994), clay minerals (Goring and Bartholomew, 1951)  
49    and soil organic matter (SOM) (McKercher and Anderson, 1989), or form insoluble precipitates with cations (Celi  
50    and Barberis, 2007). These processes lead to the stabilisation of IP in soil resulting in its accumulation and reduced  
51    bioavailability (Turner et al., 2002). In contrast, the sources and mechanisms controlling the flux of *scyllo*-, *neo*-  
52    and D-*chiro*-IP<sub>6</sub> in soil remain unknown but are thought to involve epimerization of the *myo* stereoisomer  
53    (L'Annunziata, 1975).

54    Chromatographic separation of alkaline soil extracts revealed the presence of four stereoisomers of IP<sub>6</sub> and lower-  
55    order IP<sub>1-5</sub> (Halstead and Anderson, 1970; Anderson and Malcolm, 1974; Cosgrove and Irving, 1980; Irving and  
56    Cosgrove, 1982). Irving and Cosgrove (1981) used hypobromite oxidation prior to chromatography to isolate the  
57    IP fraction in alkaline soils. The basis of this approach is that IP are considered to be highly resistant to  
58    hypobromite oxidation, whereas other organic compounds (e.g. phospholipids and nucleic acids) will undergo  
59    oxidation (Dyer and Wrenshall, 1941; Turner and Richardson, 2004). The resistance of IP to hypobromite  
60    oxidation is thought to be due to the high charge density and steric hindrance, which is caused by the chair  
61    conformation of the molecule and the bound phosphate groups, with the P in its highest oxidation state.  
62    Hypobromite oxidation of inositol (without phosphate groups) mainly results in the formation of inososes, which  
63    have an intact carbon ring (Fatiadi, 1968). Fatiadi (1968) considered that the oxidation of bromine with inositol is  
64    stereospecific and comparable to catalytic or bacterial oxidants.

65    A limitation of chromatographic separation of alkaline extracts is that there is a mixture of unknown organic  
66    compounds that can co-elute with IP, and result in an overestimation of IP concentrations (Irving and Cosgrove,  
67    1981). However, this can also occur for IP, and historically, studies often reported the combined concentration of  
68    IP<sub>6</sub> and IP<sub>5</sub> due to a lack of differentiation in their elution times (McKercher and Anderson, 1968b). More recently,

69 Almeida et al. (2018) investigated how cover crops might mobilize soil IP using hypobromite oxidation on NaOH-  
70 EDTA extracts followed by chromatographic separation. The authors found that pools of *myo*-IP<sub>6</sub> and ‘unidentified  
71 IP’ accounted for 30 % of the total extractable pool of P and hypothesised that the ‘unidentified IP’ pool consists  
72 solely of lower-order *myo*-IP. Pools of lower order IP<sub>1-5</sub> comprise on average 17 % of the total pool of IP in soil  
73 and account for an important pool of soil organic P in terrestrial ecosystems (Anderson and Malcolm, 1974;  
74 Cosgrove and Irving, 1980; Turner et al., 2002; Turner, 2007).

75 Since the 1980s, solution <sup>31</sup>P nuclear magnetic resonance spectroscopy (NMR) has been the most commonly used  
76 technique to characterise the chemical nature of organic P in soil extracts (Newman and Tate, 1980; Cade-Menun  
77 and Liu, 2014). An advantage of this technique is the simultaneous detection of all forms of organic P that come  
78 into solution, which is brought about by a single step extraction with alkali and a chelating agent (Cade-Menun  
79 and Preston, 1996). However, a limitation of the technique has been the loss of information on the diversity and  
80 amount of soil IP compared to that typically obtained prior to 1980 (Smith and Clark, 1951; Anderson, 1955;  
81 Cosgrove, 1963). To date, solution <sup>31</sup>P NMR spectroscopy on soil extracts has only reported concentrations of  
82 *myo*-, *scyllo*-, *chiro*- and *neo*-IP<sub>6</sub>. The fact that lower-order IP were not reported in studies using NMR  
83 spectroscopy might be due to overlap of peaks in the phosphomonoester region, which makes peak assignment of  
84 specific compounds difficult (Doolette et al., 2009).

85 Turner et al. (2012) carried out hypobromite oxidation prior to solution <sup>31</sup>P NMR analysis of alkaline soil extracts  
86 to isolate the IP fraction. This had the advantage of reducing the number of NMR signal in the phosphomonoester  
87 region and consequently the overlap of peaks. The authors demonstrated the presence of *neo*- and *chiro*-IP<sub>6</sub> in  
88 NMR spectra via spiking of hypobromite oxidised extracts. Interestingly, the authors also reported the presence of  
89 NMR signals in the phosphomonoester region that could not be assigned to IP<sub>6</sub> and were resistant to hypobromite  
90 oxidation. They were not able to attribute the NMR signals to any specific P compounds, but hypothesised based  
91 on their resistance to hypobromite oxidation that they were due to lower-order IP.

92 The aim of this study was to identify and quantify IP in soil extracts following hypobromite oxidation using  
93 solution <sup>31</sup>P NMR spectroscopy. In addition, the structural composition of phosphomonoesters in soil extracts  
94 following hypobromite oxidation was probed using solution <sup>31</sup>P NMR spectroscopy and transverse relaxation  
95 experiments. We hypothesise that a large portion of sharp peaks in the phosphomonoester region of untreated soil  
96 extracts would be resistant to hypobromite oxidation, which would indicate the presence of a wide variety of IP.  
97 This would have major consequences to our understanding of P cycling in terrestrial (and aquatic) ecosystems, as  
98 much more organic P compounds and mechanisms would be involved than previously thought. Furthermore, a  
99 better understanding of these organic P compounds in soil would also help improve strategies to increase their  
100 biological utilisation, which may reduce the amount of fertiliser needed in agricultural systems and thus influence  
101 the transfer of P to aquatic/marine ecosystems.

## 102 2 Experimental section

### 103 2.1 Soil collection and preparation

104 Soil samples were collected from the upper horizon of the profile at four diverse sites. These include a Ferralsol  
105 from Colombia, a Vertisol from Australia, a Cambisol from Germany, and a Gleysol from Switzerland (FAO,  
106 2014). The four soil samples were chosen from a larger collection based on their diverse concentration of P<sub>org</sub> and  
107 composition of the phosphomonoester region in NMR spectra (Reusser et al., 2020). Background information and

108 some chemical properties of the soils are reported in Table 1. Briefly, the Ferralsol was collected from an improved  
109 grassland in 1997 at the Carimagua Research Station's long-term Culticore field experiment in Columbia (Bühler  
110 et al., 2003). The Vertisol was collected from an arable field in 2018 located in southern Queensland. The site had  
111 been under native shrubland prior to 1992. The Cambisol was collected from a beech forest in 2014, and is part of  
112 the "SPP 1685 – Ecosystem Nutrition" project (Bünemann et al., 2016; Lang et al., 2017). The Gleysol was  
113 collected from the peaty top soil layer of a drained marshland in 2017, which has been under grassland for at least  
114 20 years.

115 Soil samples were passed through a 5 mm sieve and dried at 60°C for 5 days, except for the Ferralsol (sieved <2  
116 mm) and the Vertisol (ground <2 mm), which were received dried. Total concentrations of C and N in soils were  
117 obtained using combustion of 50 mg ground soil (to powder) weighed into tin foil capsules (vario PYRO cube®,  
118 Elementar Analysesysteme GmbH). Soil pH was measured in H<sub>2</sub>O with a soil to solution ratio of 1:2.5 (w/w) using  
119 a glass electrode.

120 [Suggested location Table 1]

## 121 **2.2 Soil phosphorus analyses**

122 Total concentrations of soil P were carried out by X-ray fluorescence spectroscopy (SPECTRO XEPOS ED-XRF,  
123 AMETEK®) using 4.0 g of ground to powder soil sample mixed with 0.9 g of wax (CEREOX Licowax,  
124 FLUXANA®). The XRF instrument was calibrated using commercially available reference soils. Concentrations  
125 of organic P for NMR analysis were carried out using the NaOH-EDTA extraction technique of Cade-Menun et  
126 al. (2002) at a soil to solution ratio of 1:10, i.e. extracting 4 g of soil with 40 mL of extractant.

## 127 **2.3 Hypobromite oxidation**

128 Hypobromite oxidation of NaOH-EDTA soil filtrates was carried out based on a modified version of the method  
129 described in Suzumura and Kamatani (1993) and Turner et al. (2012). The hypobromite oxidation procedure is  
130 similar to that reported in Turner (2020). Briefly, 10 mL of the NaOH-EDTA filtrate (section 2.2) was placed in a  
131 three necked round bottom flask equipped with a septum, a condenser, a magnetic stir bar and thermometer  
132 (through a claisen adapter with N<sub>2</sub> adapter). After the addition of 1 mL 10 M aqueous NaOH and vigorous stirring,  
133 an aliquot of 0.6 mL Br<sub>2</sub> (which was cooled prior to use) was added, resulting in an exothermic reaction where  
134 some of the soil extracts nearly boiled. The optimal volume of Br<sub>2</sub> for oxidation was assessed in a previous pilot  
135 study using 0.2, 0.4, 0.6 and 0.8 mL Br<sub>2</sub> volumes, and then observing differences in their NMR spectral features  
136 (Figure SI9). The reaction was heated to 100 °C within 10 min and kept at reflux for an additional 5 min. After  
137 cooling to room temperature, the solution was acidified with 2 mL of 6 M aqueous HCl solution in order to obtain  
138 a pH < 3, which was confirmed with a pH test strip. The acidified solution was reheated to 100 °C for 5 min under  
139 a stream of nitrogen to vaporise any excess bromine. The pH of the solution was gradually increased to 8.5 using  
140 10 M aqueous NaOH solution. After dilution with 10 mL of H<sub>2</sub>O, 5 mL 50 % (w/w) ethanol and 10 mL 10 % (w/w)  
141 barium acetate solution was added to the solution in order to precipitate any IP (Turner et al., 2012). The solution  
142 was then heated and boiled for 10 min and allowed to cool down overnight. The solution was subsequently  
143 transferred to a 50 mL centrifuge tube and a 10 mL aliquot of 50 % (w/w) ethanol was added, manually shaken,  
144 and centrifuged at 1500 g for 15 min. The supernatant was removed and a 15 mL aliquot of 50 % (w/w) ethanol  
145 was added to the precipitate, shaken, and then centrifuged again as before. The supernatant was removed and the  
146 process repeated once more to further purify the pool of IP. Afterwards, the precipitate was transferred with 20

147 mL of H<sub>2</sub>O into a 100 mL beaker that contained a 20 mL volume (equating to a mass of 15 g) of Amberlite® IR-  
148 120 cation exchange resin beads in the H<sup>+</sup> form (Sigma-Aldrich, product no. 06428). The suspension was stirred  
149 for 15 min and then passed through a Whatman no. 42 filter paper. A 9 mL aliquot of the filtrate was frozen at  
150 – 80 °C and then lyophilised prior to NMR analysis. This resulted in 18 - 26 mg of lyophilised material across all  
151 soils. Concentrations of total P in solutions were obtained using inductively coupled plasma-optical emission  
152 spectrometry (ICP-OES). Concentrations of molybdate reactive P (MRP) were obtained using the malachite green  
153 method of Ohno and Zibilske (1991). The difference in concentrations of total P and MRP in solution is molybdate  
154 unreactive P (MUP), which is predominantly organic P for these samples. To assess the effect of hypobromite  
155 oxidation on the stability of an IP<sub>6</sub>, duplicate samples of the Cambisol and the Gleysol were spiked with 0.1 mL  
156 of a 11 mM *myo*-IP<sub>6</sub> standard. The recovery of the added *myo*-IP<sub>6</sub> following hypobromite oxidation was calculated  
157 using Eq. (1):

$$158 \text{ Spike recovery (\%)} = \frac{C_{\text{spiked}}\left(\frac{\text{mg}}{\text{L}}\right) - C_{\text{unspiked}}\left(\frac{\text{mg}}{\text{L}}\right)}{C_{\text{standard added}}\left(\frac{\text{mg}}{\text{L}}\right)}, \quad (1)$$

159 where C<sub>spiked</sub> and C<sub>unspiked</sub> are the concentrations of *myo*-IP<sub>6</sub> in NaOH-EDTA extracts following hypobromite  
160 oxidation of the spiked and unspiked samples, respectively. C<sub>standard added</sub> is the concentration of the added *myo*-IP<sub>6</sub>  
161 within the standard. As <sup>31</sup>P NMR spectroscopy of the standard revealed impurities, the concentration of *myo*-IP<sub>6</sub>  
162 in the standard was calculated based on the <sup>31</sup>P NMR spectrum.

#### 163 2.4 Sample preparation for solution <sup>31</sup>P NMR spectroscopy

164 The lyophilised material of the untreated soil extracts was prepared for solution <sup>31</sup>P NMR spectroscopy based on  
165 a modification of the methods of Vincent et al. (2013) and Spain et al. (2018). Briefly, 120 mg of lyophilised  
166 material was taken and dissolved in 600 µL of 0.25 M NaOH-0.05 M Na<sub>2</sub>EDTA solution (ratio of 1:5). However,  
167 for the Cambisol sample, this ratio resulted in a NMR spectrum that exhibited significant line broadening.  
168 Therefore, this was repeated on a duplicate sample but at a smaller lyophilised material to solution ratio (ratio of  
169 1:7.5), as suggested in Cade-Menun and Liu (2014), which resolved the issue of poor spectral quality. The  
170 suspension was stored overnight to allow for complete hydrolysis of phospholipids and RNA (Doolittle et al., 2009;  
171 Vestergren et al., 2012), which was then centrifuged at 10621 g for 15 min. A 500 µL aliquot of the supernatant  
172 was taken, which was subsequently spiked with a 25 µL aliquot of a 0.03 M methylenediphosphonic acid standard  
173 made in D<sub>2</sub>O (Sigma-Aldrich, product no. M9508) and a 25 µL aliquot of sodium deuterioxide at 40 % (w/w) in  
174 D<sub>2</sub>O (Sigma-Aldrich, product no. 372072). The solution was then mixed and transferred to a 5 mm diameter NMR  
175 tube.

176 A similar procedure was used for the soil extracts that had undergone hypobromite oxidation, except the total mass  
177 of lyophilised material (18 - 26 mg) was dissolved with 600 µL of a 0.25 M NaOH-0.05 M Na<sub>2</sub>EDTA solution.  
178 However, for the Cambisol sample, the NMR spectrum exhibited considerable line-broadening, and an additional  
179 400 µL aliquot of NaOH-EDTA solution was added to the NMR tube, mixed, and then returned to the NMR  
180 spectrometer. This resolved the issue of poor spectral quality.

#### 181 2.5 Solution <sup>31</sup>P NMR spectroscopy

182 Solution <sup>31</sup>P NMR analyses were carried out on all untreated and hypobromite oxidised soil extracts at the NMR  
183 facility of the Laboratory of Inorganic Chemistry (Hönggerberg, ETH Zürich). All spectra were obtained with a  
184 Bruker AVANCE III MD 500 MHz NMR spectrometer equipped with a cryogenic probe (CryoProbe™ Prodigy)

185 (Bruker Corporation; Billerica, MA). The  $^{31}\text{P}$  frequency for this NMR spectrometer was 202.5 MHz and gated  
186 broadband proton decoupling with a  $90^\circ$  pulse of 12  $\mu\text{s}$  was applied. Spectral resolution under these conditions for  
187  $^{31}\text{P}$  was  $< 1$  Hz. Longitudinal relaxation ( $T_1$ ) times were determined for each sample with an inversion recovery  
188 experiment (Vold et al., 1968). This resulted in recycle delays ranging from 8.7 to 30.0 sec for the untreated  
189 extracts and 7.8 to 38.0 sec for the hypobromite oxidised soil extracts. The number of scans for the untreated  
190 extracts was set to 1024 or 4096, depending on the signal to noise ratio of the obtained spectrum. All hypobromite  
191 oxidised spectra were acquired with 3700 to 4096 scans.

## 192 **2.6 Processing of NMR spectra**

193 All NMR spectra were processed with Fourier transformation, phase correction, and baseline adjustment within  
194 the TopSpin® software environment (Version 3.5 pl 7, Bruker Corporation; Billerica, MA). Line broadening was  
195 set to 0.6 Hz. Quantification of NMR signals involved obtaining the integrals of the following regions: 1) up to  
196 four phosphonates ( $\delta$  19.8 to 16.4 ppm); 2) the added MDP ( $\delta$  17.0 to 15.8 ppm) including its two carbon satellite  
197 peaks; 3) the combined orthophosphate and phosphomonoester region ( $\delta$  6.0 to 3.0 ppm); 4) up to four  
198 phosphodiesters ( $\delta$  2.5 to -3.0 ppm), and 5) pyrophosphate ( $\delta$  -4.8 to -5.4 ppm). Due to overlapping peaks in the  
199 orthophosphate and phosphomonoester region, spectral deconvolution fitting (SDF) was applied as described in  
200 Reusser et al. (2020). In brief, the SDF procedure involved the fitting of an underlying broad signal, based on the  
201 approach of Bünemann et al. (2008) and McLaren et al. (2019). We carried out the SDF with a non-linear  
202 optimisation algorithm in MATLAB® R2017a (The MathWorks, Inc.) and fitted visually identifiable peaks by  
203 constraining their line-widths at half height as well as the lower and upper boundary of the peak positions along  
204 with an underlying broad signal in the phosphomonoester region. The sharp signals of high intensity (e.g.  
205 orthophosphate) and the broad peak were fitted using Lorentzian lineshapes, whereas sharp signals of low intensity  
206 were fitted using Gaussian lineshapes. The NMR observability of total P ( $P_{\text{tot}}$ ) in NaOH-EDTA extracts was  
207 calculated using Eq. (2) (Dougherty et al., 2005; Doolette et al., 2011b):

$$208 \text{NMR observability (\%)} = \frac{P_{\text{tot NMR}}}{P_{\text{tot ICP-OES}}} * 100 \% , \quad (2)$$

209 where  $P_{\text{tot NMR}}$  refers to the total P content in mg P/kg<sub>soil</sub> detected in the soil extracts using solution  $^{31}\text{P}$  NMR  
210 spectroscopy and  $P_{\text{tot ICP-OES}}$  refers to the total P concentration in mg P/kg<sub>soil</sub> measured in the soil extracts prior  
211 to freeze-drying using ICP-OES.

## 212 **2.7 Spiking experiments**

213 To identify the presence of IP in hypobromite oxidised extracts, samples were spiked with a range of standards  
214 and then analysed again using NMR spectroscopy. This involved the addition of 5 to 20  $\mu\text{L}$  aliquots of an IP  
215 standard solution directly into the NMR tube, which was then sealed with parafilm, manually shaken, and then  
216 allowed to settle prior to NMR analysis. Each sample extract was consecutively spiked with no more than four IP  
217 standards. The NMR spectra of soil extracts after spiking were overlaid with the NMR spectra of unspiked soil  
218 extracts to identify the presence of IP across all soil samples. This comparison of NMR spectra was possible due  
219 to negligible changes in the chemical shifts of peaks among soil samples. The IP standards used in this study are  
220 listed in Table 2.

221 [Suggested location Table 2]

222 **2.8 Transverse relaxation ( $T_2$ ) experiments**

223 Due to the presence of sharp and broad signals in the phosphomonoester region of NMR spectra on hypobromite  
224 oxidised soil extracts, transverse relaxation ( $T_2$ ) experiments were carried out to probe their structural composition.  
225 The transverse relaxation (originally spin-spin relaxation) describes the loss of magnetisation in the x-y plane. This  
226 loss occurs due to magnetic field differences in the sample, arising either by instrumentally caused magnetic field  
227 inhomogeneities or by local magnetic fields in the sample caused by intramolecular and intermolecular interactions  
228 (Claridge, 2016). Generally, small, rapidly tumbling molecules exhibit longer  $T_2$  relaxation times compared to  
229 large, slowly tumbling molecules (McLaren et al., 2019).

230 Briefly, solution  $^{31}\text{P}$  NMR spectroscopy with a Carr-Purcell-Meiboom-Gill (CPMG) pulse sequence (Meiboom  
231 and Gill, 1958) was carried out on all hypobromite oxidised soil extracts, as described in McLaren et al. (2019).  
232 This involved a constant spin-echo delay ( $\tau$ ) of 5 ms, which was repeated for a total of eight iterations (spin-echo  
233 periods of 5, 50, 100, 150, 200, 250, 300, and 400 ms). A total of 4096 scans and a recycle delay of 4.75 sec was  
234 used for all iterations. Transverse relaxation times for the aforementioned integral ranges were calculated using  
235 Eq. (3) within the TopSpin® software environment. Due to overlapping peaks in the orthophosphate and  
236 phosphomonoester region, spectral deconvolution was carried out to partition the NMR signal, as described in  
237 McLaren et al. (2019). The  $T_2$  times of the partitioned NMR signals were calculated using Eq. (3) within RStudio©  
238 (version 1.1.442):

$$239 M(t) = M_0 * e^{(-t*T_2^{-1})}, \quad (3)$$

240 where  $M$  refers to the net magnetisation derived from the average angular momentum in the x-y plane,  $\tau$  refers to  
241 the spin-echo delay in milliseconds (ms), and  $T_2$  refers to the transverse relaxation time (ms).

242 **2.9 Statistical analyses and graphics**

243 Statistical analyses were carried out using Microsoft® Excel 2016 and MATLAB R2017a (©The MathWorks,  
244 Inc.). Graphics were created with Microsoft® Excel 2016 and MATLAB R2017a (©The MathWorks, Inc.).  
245 Solution (1D)  $^{31}\text{P}$  NMR spectra were normalised to the peak intensity of MDP ( $\delta$  16.46 ppm). Spectra from the  $T_2$   
246 experiments were normalised to the peak intensity of *scyllo*-IP<sub>6</sub> ( $\delta$  3.22 ppm).

247 A one-way ANOVA was carried out in MATLAB R2017a (©The MathWorks, Inc.) with a subsequent multi  
248 comparison of mean values using the Tukey's honestly significant difference procedure based on the studentised  
249 range distribution (Hochberg and Tamhane, 1987; Milliken and Johnson, 2009).

250 **3 Results**

251 **3.1 Phosphorus concentrations in soil extracts**

252 Concentrations of total soil P as determined by XRF ranged from 320 to 3841 mg P/kg<sub>soil</sub> across all soils (Table  
253 3). Concentrations of total P as estimated by the NaOH-EDTA extraction technique ranged from 160 to  
254 1850 mg P/kg<sub>soil</sub>, which comprised 28 to 51 % of the total soil P as determined by XRF. Pools of organic P  
255 comprised 28 to 72 % of the total P in NaOH-EDTA untreated soil extracts.

256 Concentrations of total P in NaOH-EDTA soil extracts following hypobromite oxidation ranged from 77 to 578 mg  
257 P/kg<sub>soil</sub> (Table 3), which accounted for 31 to 48 % (on average 38 %) of the total P originally present in the extracts.  
258 Similarly, pools of organic P in NaOH-EDTA extracts following hypobromite oxidation were lower, comprising  
259 22 to 48 % (on average 36 %) of that originally present in untreated NaOH-EDTA extracts across all soils.

260 [Suggested location Table 3]

261 **3.2 Solution  $^{31}\text{P}$  NMR spectra of hypobromite oxidised soil extracts**

262 The most prominent signal in the NMR spectra of untreated NaOH-EDTA soil extracts was that of orthophosphate  
263 at  $\delta$  5.25 ( $\pm 0.25$ ) ppm, followed by the phosphomonoester region ranging from  $\delta$  6.0 to 3.0 ppm (Fig. 1). There  
264 were also some minor signals due to pyrophosphate  $\delta$  -5.06 ( $\pm 0.19$ ) ppm (all soils), phosphodiesters ranging from  
265  $\delta$  2.5 to -2.4 ppm (not detected in the Vertisol), and phosphonates (not including the added MDP) at  $\delta$  19.8, 19.2  
266 and 18.3 ppm (not detected in the Gleysol). However, these compounds comprised less than 8 % of the total NMR  
267 signal.

268 Following hypobromite oxidation of NaOH-EDTA extracts, the most prominent NMR signals were found in the  
269 orthophosphate (65 % of total NMR signal) and phosphomonoester (35 % of total NMR signal) region across all  
270 soils (Fig. 1). Phosphodiesters and pyrophosphates were removed following hypobromite oxidation in the  
271 Ferralsol, the Vertisol and the Cambisol (DE). However, some signal remained in the Gleysol at low concentrations  
272 (0.4 % of the total NMR signal). Phosphonates were removed following hypobromite oxidation in the Ferralsol  
273 and the Vertisol, but a total of five sharp peaks in the phosphonate region were detected ( $\delta$  19.59, 18.58, 17.27 and  
274 9.25 ppm) in the Cambisol. These peaks comprised 0.6 % of the total NMR signal.

275 The phosphomonoester region of NMR spectra on untreated NaOH-EDTA extracts exhibited two main features:  
276 1) the presence of a broad signal centered at around  $\delta$  4.1 ( $\pm 0.1$ ) ppm with an average line-width at half height of  
277 256.12 Hz; and 2) the presence of between 19 and 34 sharp signals. This was similarly the case on hypobromite  
278 oxidised extracts, except there was a decrease in the intensity of the broad signal and a change in the distribution  
279 and intensity of sharp signals. For the Cambisol and Gleysol, the number of sharp signals in the phosphomonoester  
280 region approximately doubled (to 40 and 70 sharp signals, respectively) following hypobromite oxidation. In  
281 contrast, less than half of the sharp signals remained in the Ferralsol following hypobromite oxidation (i.e. 14 of  
282 the 30 peaks originally present in the untreated extract), whereas one peak was removed following hypobromite  
283 oxidation in the Vertisol. There was little change (0.23 ppm) in the chemical shifts of peaks between the untreated  
284 and hypobromite oxidised extracts.

285

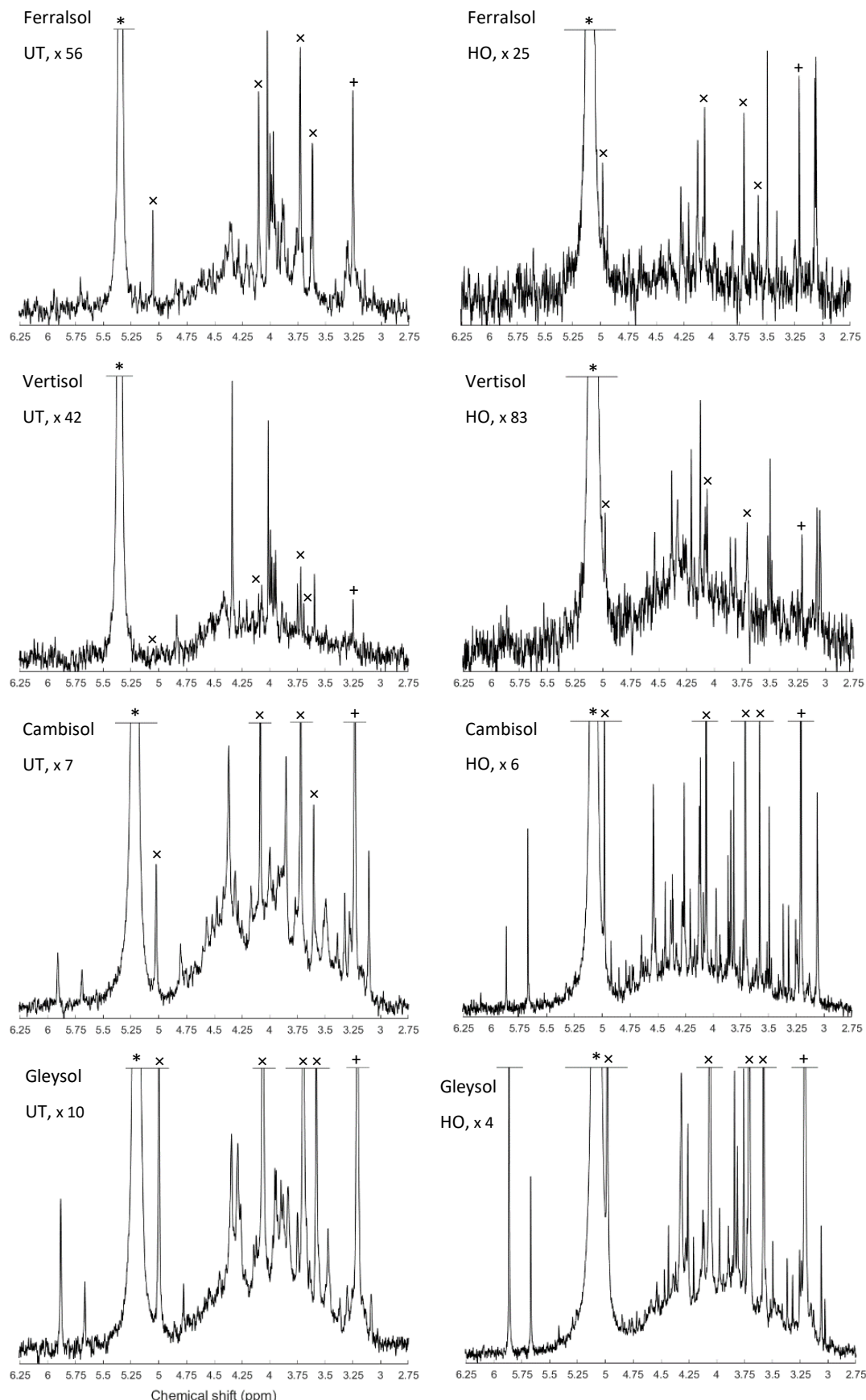


**Figure 1.** Solution  $^{31}\text{P}$  nuclear magnetic resonance (NMR) spectra (500 MHz) of the orthophosphate and phosphomonoester region on untreated (UT) and hypobromite oxidised (HO) 0.25 M NaOH + 0.05 M EDTA soil extracts (Ferralsol, Vertisol, Cambisol and Gleysol). Signal intensities were normalised to the MDP peak intensity. The vertical axes were increased for improved visibility of spectral features, as indicated by a factor. The orthophosphate peak is marked with an asterisk. The symbol 'x' marks the four individual peaks of *myo*-IP<sub>6</sub> and '+' the peak of *scyllo*-IP<sub>6</sub>.

287 [Suggested location Table 4]

288 **3.3 Identification and quantification of inositol phosphates (IP<sub>6</sub>, IP<sub>5</sub> and IP<sub>4</sub>) in soil extracts**

289 Detailed views of the phosphomonoester regions of spiked samples are shown in Fig. SI1 to SI5 of the Supporting  
290 Information. The number of identified sharp peaks in the phosphomonoester region ranged from 7 (Vertisol) to 33  
291 (Gleysol). *myo*- and *scyllo*-IP<sub>6</sub> were identified in the hypobromite oxidised extracts of all soils (Table 5). On  
292 average, 72 % of *myo*-IP<sub>6</sub> and 56 % of *scyllo*-IP<sub>6</sub> present in the untreated extracts remained in the hypobromite  
293 oxidised extracts (Table SI1 in the Supporting Information). *neo*-IP<sub>6</sub> was identified in the the 2-equatorial/4-axial  
294 and 4-equatorial/2-axial conformations, and *chiro*-IP<sub>6</sub> in the 2-equatorial/4-axial confirmation, of the oxidised  
295 extracts in the Cambisol and Gleysol, but were absent in the Ferralsol and the Vertisol (Fig. SI4 and SI5 in the  
296 Supporting Information).

297 The *myo*, *scyllo*, *chiro* and *neo* stereoisomers of IP<sub>5</sub> were identified in various hypobromite oxidised extracts (Table  
298 5). Two isomers of *myo*-IP<sub>5</sub> were identified in some extracts, which included *myo*-(1,2,4,5,6)-IP<sub>5</sub> and *myo*-  
299 (1,3,4,5,6)-IP<sub>5</sub>. In addition, *scyllo*-IP<sub>4</sub> was detected in all soils except that of the Vertisol. There was insufficient  
300 evidence for the presence of *myo*-IP<sub>4</sub> in these soil samples, as only one of the two peaks of this compound was  
301 present in the NMR spectra of untreated extracts. This could possibly be due to the partial dephosphorylation of  
302 *myo*-IP<sub>4</sub> during the hypobromite oxidation procedure. The reason of the reduced resistance of lower order IP to  
303 hypobromite oxidation compared to IP<sub>5+6</sub> might be due to their reduced steric hindrance and charge density, as less  
304 phosphate groups are bound to the inositol ring.

305 Concentrations of total IP ranged from 1.4 to 159.3 mg P/kg<sub>soil</sub> across all soils, which comprised between 1 %  
306 (Vertisol) and 18 % (Gleysol) of the organic P in untreated NaOH-EDTA extracts (Table 3). Pools of IP<sub>6</sub> were the  
307 most abundant form of IP, which ranged from 0.9 to 144.8 mg P/kg<sub>soil</sub> across all soils (Table 5). The proportion of  
308 IP<sub>6</sub> stereoisomers across all soils were in the order of *myo* (61 %, SD=12), *scyllo* (29 %, SD=3), *chiro* (6 %, SD=8)  
309 and *neo* (4 %, SD=5). Similarly, the *myo* and *scyllo* stereoisomer were also the most predominant forms of IP<sub>5</sub>,  
310 but comprised between 83 % (Cambisol) and 100 % (Ferralsol and Vertisol) of total IP<sub>5</sub> (Table 5). Trace amounts  
311 of *scyllo*-IP<sub>4</sub> were also detected in three of the four soils. The ratio of total IP<sub>6</sub> to IP<sub>5</sub> differed across all soils (Fig.  
312 2).

313 [Suggested location Table 5]

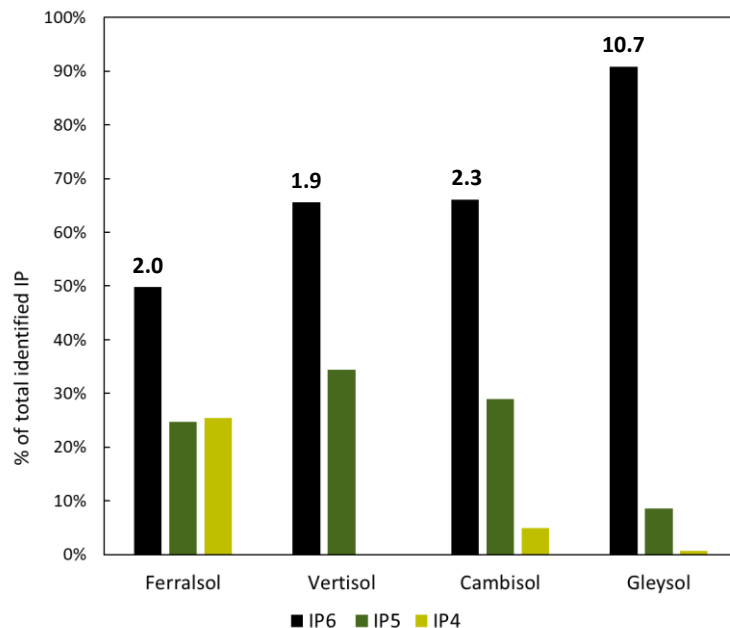


**Figure 2.** The proportion of total identifiable pools of inositol hexakisphosphates (IP<sub>6</sub>), -pentakisphosphates (IP<sub>5</sub>) or -tetrakisphosphates (IP<sub>4</sub>) to that of the total pool of identifiable IP, as determined by solution <sup>31</sup>P NMR spectroscopy on four soil extracts (Ferralsol, Vertisol, Cambisol and Gleysol) following hypobromite oxidation. Values located above the IP<sub>6</sub> bar are the ratio of total identifiable IP<sub>6</sub> to that of IP<sub>5</sub> in each soil sample.

314

315 If sharp peaks arising from IP were identified in the NMR spectra on hypobromite oxidised extracts, a comparison  
 316 was made with that of their corresponding untreated extracts. The sharp peaks of all stereoisomers of IP<sub>6</sub> were  
 317 present in the untreated extracts. The five peaks of *myo*-(1,2,4,5,6)-IP<sub>5</sub> and the three peaks of *scyllo*-IP<sub>5</sub> were also  
 318 identified. However, it was not possible to clearly identify other IP<sub>5</sub> compounds in untreated extracts due to  
 319 overlapping signals. In the Gleysol, all three peaks of *scyllo*-IP<sub>5</sub> were detected, but only two of the possible five  
 320 peaks could be clearly assigned to *myo*-(1,2,4,5,6)-IP<sub>5</sub>. In the Ferralsol, both peaks of *scyllo*-IP<sub>4</sub> were present in  
 321 the untreated extract, but only two of the three possible peaks could be assigned to *scyllo*-IP<sub>5</sub>. In the Vertisol, no  
 322 IP<sub>5</sub> was identified. Concentrations of IP in untreated extracts assessed by spectral deconvolution fitting were  
 323 generally double than that measured in hypobromite oxidised extracts. Recoveries of added *myo*-IP<sub>6</sub> in the Gleysol  
 324 and Cambisol following hypobromite oxidation were 47 % and 20 %, respectively.

325 **3.4 Spin-echo analysis of selected P compounds**

326 Due to the presence of sharp and broad signals in hypobromite oxidised soil extracts, the structural composition  
 327 of phosphomonoesters was probed. A comparison of the NMR spectra at the lowest (1\* $\tau$ ) and highest (80\* $\tau$ ) pulse  
 328 delays revealed a fast decaying broad signal for all hypobromite oxidised soil extracts, which was particularly  
 329 evident in the Gleysol (Fig. 3). Calculated T<sub>2</sub> times of all IP<sub>6</sub> stereoisomers were longer than that of the broad  
 330 signal (Table 6). The T<sub>2</sub> times of *scyllo*-IP<sub>6</sub> (on average 175.8 ms, SD=49.7) were generally the longest of all  
 331 stereoisomers of IP<sub>6</sub>. The T<sub>2</sub> time of the orthophosphate peak was the shortest, which was on average 11.5 ms  
 332 (SD=4.9).

333 The average (n=4) T<sub>2</sub> times of the broad peak was significantly different than that of *scyllo*- and *myo*-IP<sub>6</sub> (p <  
 334 0.05). Significant differences in the T<sub>2</sub>-times of *neo*- and *D-chiro*-IP<sub>6</sub> were not tested, as these compounds were  
 335 not detected in the Ferralsol and the Vertisol.

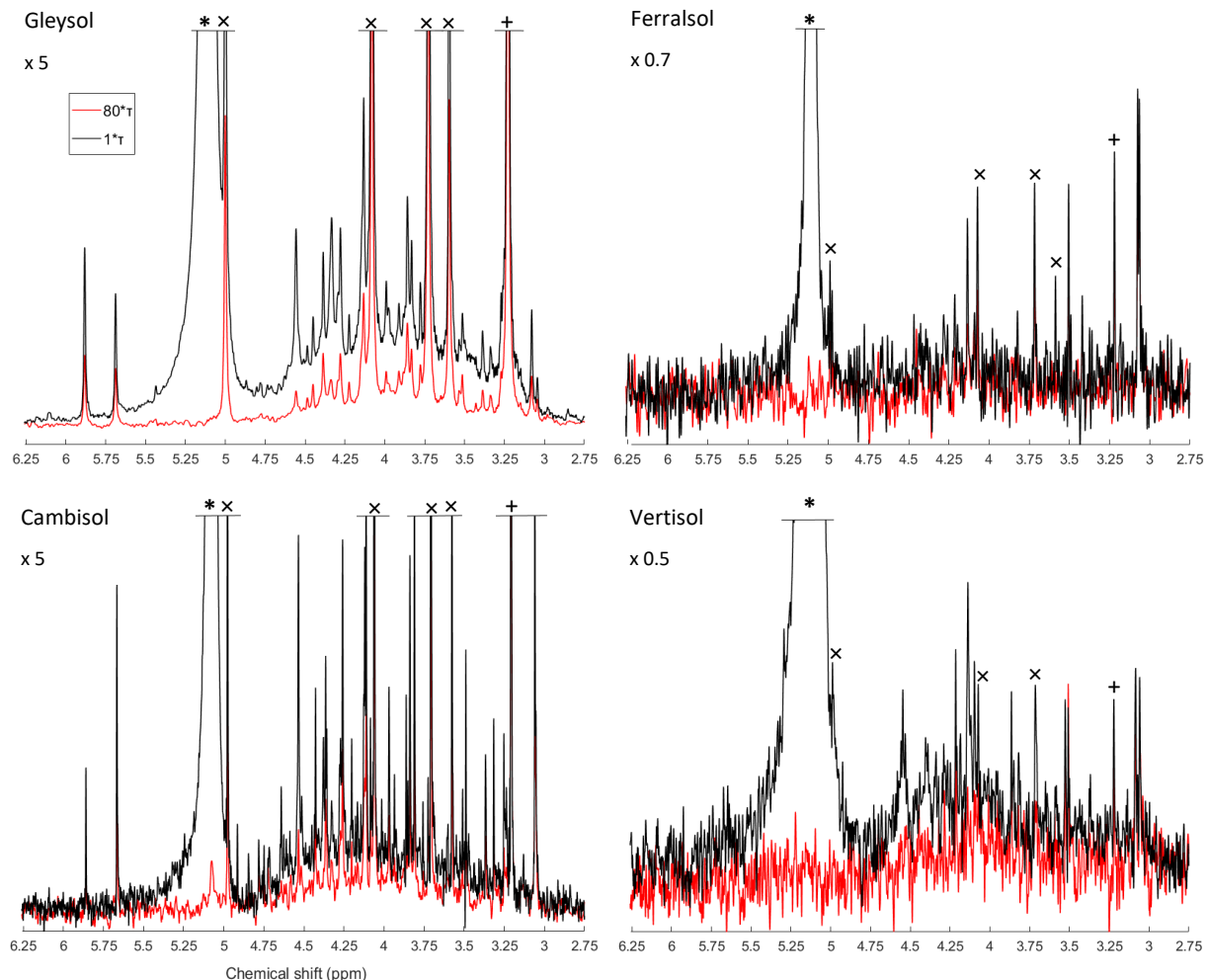


**Figure 3. Solution  $^{31}\text{P}$  NMR spectra of hypobromite oxidised soil extracts acquired with a CPMG pulse sequence with  $1^*\tau$  (black) and  $80^*\tau$  (red) spin-echo delays. The orthophosphate (\*), scyllo-IP<sub>6</sub> (+) and myo-IP<sub>6</sub> peaks (x) are marked accordingly. Spectra were normalised to the maximum scyllo-IP<sub>6</sub> peak intensity in the  $1^*\tau$  spectrum for each soil. The vertical axes were increased/decreased for better visualisation by an indicated factor.**

## 338 4 Discussion

## 339 4.1 Pools of phosphorus in untreated and hypobromite oxidised soil extracts

340 On average, 44 % of total P (as measured with XRF) was extracted by NaOH-EDTA, which is consistent with  
 341 previous studies (Turner, 2008; Li et al., 2018; McLaren et al., 2019). The non-extractable pool of P is likely to  
 342 comprise of inorganic P as part of insoluble mineral phases, but could also contain some organic P (McLaren et  
 343 al., 2015a). Nevertheless, the NaOH-EDTA extraction technique is considered to be a measure of total organic P  
 344 in soil, which can be subsequently characterised by solution  $^{31}\text{P}$  NMR spectroscopy (Cade-Menun and Preston,  
 345 1996).

346 Hypobromite oxidation resulted in a decrease in the concentration of inorganic and organic P in NaOH-EDTA  
 347 extracts across all soils. The decrease of organic P is consistent with previous studies (Turner and Richardson,  
 348 2004; Turner et al., 2012; Almeida et al., 2018). However, Almeida et al. (2018) reported an overall increase in  
 349 the concentration of inorganic P following hypobromite oxidation, which the authors proposed to be caused by the

350 degradation of organic P forms not resistant to hypobromite oxidation. A decrease in the concentration of organic  
351 P in NaOH-EDTA extracts following hypobromite oxidation was expected based on the oxidation of organic  
352 molecules containing P. The products of hypobromite oxidation are most probably carbon dioxide, simple organic  
353 acids from the oxidative cleavage of the phosphoesters and orthophosphate (Irving and Cosgrove, 1981; Sharma,  
354 2013).

355 Overall, hypobromite oxidation of NaOH-EDTA soil extracts resulted in a considerable increase in the number of  
356 sharp peaks and a decrease in the broad underlying peak in the phosphomonoester region compared to that of  
357 untreated soil extracts. This was particularly the case for the Cambisol and the Gleysol, which had high  
358 concentrations of extractable organic P. Since the broad peak is thought to be closely associated with the SOM  
359 (Dougherty et al., 2007; Bünemann et al., 2008; McLaren et al., 2015b), its decrease in soil extracts following  
360 hypobromite oxidation is consistent with that observed for other organic compounds (Turner et al., 2012). Our  
361 results indicate that the majority of sharp peaks present in the phosphomonoester region of untreated soil extracts  
362 are stable to hypobromite oxidation, and are therefore likely to be IP.

363 Across all soils, 5 to 15 peaks in the phosphomonoester region were removed following hypobromite oxidation  
364 compared to those in untreated extracts, which are likely due to the oxidation of:  $\alpha$ -and  $\beta$ -glycerophosphate  
365 (Doolette et al., 2009; McLaren et al., 2015b), RNA mononucleotides (8 peaks) (Vincent et al., 2013), glucose 6-  
366 phosphate, phosphocholine, glucose 1-phosphate, or phosphorylethanolamine (Cade-Menun, 2015).

#### 367 **4.2 Phosphorus assignments of sharp peaks in hypobromite oxidised extracts**

368 The detection of *myo*-, *scyllo*-, *chiro*, and *neo*-IP<sub>6</sub> in untreated and hypobromite oxidised soil extracts is consistent  
369 with previous studies using chromatography (Irving and Cosgrove, 1982; Almeida et al., 2018) and NMR (Turner  
370 and Richardson, 2004; Doolette et al., 2011a; Vincent et al., 2013; Jarosch et al., 2015; McLaren et al., 2015b).  
371 Turner et al. (2012) suggested that hypobromite oxidised extracts only contained *neo*-IP<sub>6</sub> in the 4-equatorial/2-  
372 axial conformation due to the absence of signals from the 2-equatorial/4-axial conformation. In the current study,  
373 both conformations could be identified in two of the four soil extracts, which is likely due to improved spectral  
374 resolution and sensitivity. The relative abundances of the four identified stereoisomers of IP<sub>6</sub> in soil extracts were  
375 similar to previous studies (Irving and Cosgrove, 1982; Turner et al., 2012).

376 Several studies have shown overlap of peaks relating to RNA mononucleotides and that of  $\alpha$ -and  $\beta$ -  
377 glycerophosphate, which are the alkaline hydrolysis products of RNA and phospholipids, respectively. However,  
378 in the current study, several sharp peaks were present in hypobromite oxidised extracts which are in the chemical  
379 shift range of RNA mononucleotides and  $\alpha$ -and  $\beta$ -glycerophosphate. Whilst a peak at  $\delta$  4.36 ppm would be  
380 assigned to  $\alpha$ -glycerophosphate based on spiking experiments in the untreated extracts of the Cambisol and the  
381 Gleysol, hypobromite oxidation revealed the presence of the 2-equatorial/4-axial C2,5 peak of *neo*-IP<sub>6</sub> at  $\delta$   
382 4.37 ppm, and also an unidentified peak at  $\delta$  4.36 ppm in the Cambisol. Therefore, the assignment and  
383 concentration of  $\alpha$ -glycerophosphate may be unreliable in some soils of previous studies.

384 For the first time, we identified lower-order IP (IP<sub>5</sub> and IP<sub>4</sub>) in soil extracts using solution <sup>31</sup>P NMR spectroscopy.  
385 Smith and Clark (1951) were the first to suggest the presence of IP<sub>5</sub> in soil extracts using anion-exchange  
386 chromatography, which was later confirmed (Anderson, 1955; Cosgrove, 1963; McKercher and Anderson, 1968b).  
387 Halstead and Anderson (1970) reported the presence of all four stereoisomers (*myo*, *scyllo*, *neo* and *chiro*) in the  
388 lower ester fractions (IP<sub>2</sub>-IP<sub>4</sub>) as well as the higher ester fractions (IP<sub>5</sub>, IP<sub>6</sub>) isolated from soil, with the *myo*  
389 stereoisomer being the main form in all fractions. In the current study, all four stereoisomers of IP<sub>5</sub> could be

390 detected in the hypobromite oxidised soil extracts, of which the *myo* and *scyllo* stereoisomers were the most  
391 abundant. The relative abundances of IP<sub>5</sub> stereoisomers are consistent with the findings of Irving and Cosgrove  
392 (1982) using gas-liquid chromatography on the combined IP<sub>6</sub> + IP<sub>5</sub> fraction. The detection of all four stereoisomers  
393 of IP<sub>5</sub> in NMR spectra provides direct spectroscopic evidence for their existence in soil extracts.

394 In addition to the four stereoisomers of IP<sub>5</sub>, we were able to identify the presence of two isomers of *myo*-IP<sub>5</sub> in the  
395 Cambisol and Gleysol, i.e. *myo*-(1,2,4,5,6)-IP<sub>5</sub> and *myo*-(1,3,4,5,6)-IP<sub>5</sub>. These two isomers have not yet been  
396 detected in soil extracts. A distinction of different *myo*-IP<sub>5</sub> isomers was not reported in earlier studies using  
397 chromatographic separation. In non-soil extracts, *myo*-(1,2,4,5,6)-IP<sub>5</sub> was detected by Doolette and Smernik  
398 (2016) in grapevine canes, and *myo*-(1,3,4,5,6)-IP<sub>5</sub> as the thermal decomposition product of a phytate standard  
399 (Doolette and Smernik, 2018). It is possible that an abiotic transformation of *myo*-IP<sub>6</sub> to *myo*-(1,3,4,5,6)-IP<sub>5</sub> occurs,  
400 which could then be adsorbed by soil constituents. Stephens and Irvine (1990) reported *myo*-(1,3,4,5,6)-IP<sub>5</sub> as an  
401 intermediate in the synthesis of IP<sub>6</sub> from *myo*-IP in the cellular slime mould *Dictyostelium*. Therefore, *myo*-  
402 (1,3,4,5,6)-IP<sub>5</sub> could have been biologically added to the soil. Furthermore, *myo*-(1,3,4,5,6)-IP<sub>5</sub> was present in  
403 different animal feeds and manures (Sun and Jaisi, 2018). Sun et al. (2017) reported *myo*-(1,3,4,5,6)-IP<sub>5</sub> and *myo*-  
404 (1,2,4,5,6)-IP<sub>5</sub> as intermediates in the minor, resp. major pathways of *Aspergillus niger* phytase and acid  
405 phosphatase (potato) phytate degradation. The presence of *myo*-(1,2,3,4,6)-IP<sub>5</sub> could not be confirmed as NMR  
406 analyses on the compound itself exhibited a broad NMR signal (Fig. SI7 in the Supporting Information). This is  
407 because in solutions with a pH of 9.5 or above, the 1-axial/5-equatorial and 5-axial/1-equatorial forms of *myo*-  
408 (1,2,3,4,6)-IP<sub>5</sub> are in a dynamic equilibrium, which can cause broadening (Volkmann et al., 2002). According to  
409 Turner and Richardson (2004) and Chung et al. (1999), the two identified *scyllo*-IP<sub>4</sub> peaks (signal pattern 2:2) can  
410 be attributed to the *scyllo*-(1,2,3,4)-IP<sub>4</sub> isomer. However, the two peaks of *scyllo*-IP<sub>4</sub> overlapped in the Cambisol  
411 and Gleysol with the peak at the furthest upfield chemical shift of *myo*-(1,2,4,5,6)-IP<sub>5</sub> at  $\delta$  3.25 ppm, and with the  
412 peak at the furthest downfield chemical shift of *myo*-(1,3,4,5,6)-IP<sub>5</sub> at  $\delta$  4.12 ppm. Turner and Richardson (2004)  
413 reported NMR-signals for two other *scyllo*-IP<sub>4</sub> isomers, which could not be tested for in this study due to the lack  
414 of available standards.

415 Whilst on average 48 % of the sharp peaks in the phosphomonoester region of soil extracts following hypobromite  
416 oxidation could be attributed to IP<sub>6</sub>, IP<sub>5</sub> and *scyllo*-IP<sub>4</sub>, the identity of many sharp peaks remain unknown. An  
417 unidentified peak at  $\delta$  4.33 ppm is present in all soil samples except in the Ferralsol, with concentrations of up to  
418 10 mg P/kg<sub>soil</sub> (Cambisol). Other unidentified peaks at  $\delta$  3.49, 3.86, 4.20 and 3.91 ppm were detected in all soils,  
419 with concentrations ranging from 1 to 2 mg P/kg<sub>soil</sub>. Interestingly, two peaks upfield of *scyllo*-IP<sub>6</sub> became more  
420 prominent (at  $\delta$  3.08, 3.05 ppm) following hypobromite oxidation, which was particularly the case in the Vertisol  
421 soil. The diversity of organic P species in the Vertisol soil appears to be much greater than previously reported  
422 (McLaren et al., 2014). We hypothesise that many of these unidentified peaks arise from other isomers of *myo*-  
423 and *scyllo*-IP<sub>5</sub>, based on the higher abundance of their IP<sub>6</sub> counterparts.

424 The ratio of IP<sub>6</sub> to lower-order IP varied across soils, which ranged in decreasing order: Gleysol  $\gg$  Cambisol >  
425 Vertisol > Ferralsol. McKercher and Anderson (1968a) found a higher ratio of IP<sub>6</sub> to IP<sub>5</sub> in some Scottish soils  
426 (ratio 1.8 to 4.6) compared to some Canadian soils (0.9 to 2.4). The authors attributed this difference to the greater  
427 stabilization of IP<sub>6</sub> relative to lower esters in the Scottish soils, possible due to climatic reasons or effects of  
428 different soil properties. In a subsequent study, McKercher and Anderson (1968b) observed increased IP contents  
429 with increasing total organic P content. Studies of organic P speciation along chronosequences found that *myo*-IP<sub>6</sub>  
430 concentrations declined in older soils (McDowell et al., 2007; Turner et al., 2007a; Turner et al., 2014). Similarly,

431 Baker (1976) found that the IP<sub>6</sub> + IP<sub>5</sub> concentrations in the Franz Josef chronosequence increased until 1000 years,  
432 followed by a rapid decline. In our soil samples, the highest IP<sub>6</sub> to IP<sub>5</sub> ratio was found in the soil with the highest  
433 SOM content, suggesting a possible stabilization of IP<sub>6</sub> due to association with SOM (Borie et al., 1989; Makarov  
434 et al., 1997). In contrast, the Ferralsol sample containing high amounts of Fe and Al showed the smallest IP<sub>6</sub> to IP<sub>5</sub>  
435 ratio, even though IP<sub>6</sub> is known to strongly adsorb to sesquioxides (Anderson and Arlidge, 1962; Anderson et al.,  
436 1974). However, the production, input and mineralisation rates of IP<sub>6</sub> and IP<sub>5</sub> are not known for our soil samples.  
437 Further research is needed to understand the mechanisms controlling the flux of lower-order IP in soil.  
438 In the Ferralsol and the Cambisol, there was an overall decrease in the concentration of IP<sub>6</sub> and IP<sub>5</sub> following  
439 hypobromite oxidation compared to the untreated extracts. Since the main cause of resistance of IP to hypobromite  
440 oxidation is that of steric hindrance, which generally decreases with decreasing phosphorylation state and  
441 conformation of the phosphate groups (axial vs. equatorial), we assume that low recoveries of added *myo*-IP<sub>6</sub> is  
442 due to losses of precipitated P<sub>org</sub> compounds during the precipitation and dissolution steps. This is supported by  
443 the decrease in the concentration of orthophosphate following hypobromite oxidation compared to untreated  
444 extracts. Therefore, quantities of IP as reported in the current study should be considered as conservative.

#### 445 4.3 Structural composition of phosphomonoesters in hypobromite oxidised soil extracts

446 The NMR spectra on hypobromite oxidised soil extracts revealed the presence of sharp and broad signals in the  
447 phosphomonoester region. Transverse relaxation experiments revealed a rapid decay of the broad signal compared  
448 to the sharp peaks of IP<sub>6</sub>, which support the hypothesis that the compounds causing the broad signal arise from P  
449 compounds other than IP. These findings are consistent with that of McLaren et al. (2019), who probed the  
450 structural composition of phosphomonoesters in untreated soil extracts. Overall, measured T<sub>2</sub> times in the current  
451 study on hypobromite oxidised extracts were markedly longer compared to that on untreated extracts reported in  
452 McLaren et al. (2019). This could be due to removal of other organic compounds by hypobromite oxidation in the  
453 matrix and therefore a decrease in the viscosity of the sample. This would result in an overall faster tumbling of  
454 the molecules and hence an increased T<sub>2</sub> relaxation time. As reported by McLaren et al. (2019), calculations of the  
455 broad signal's linewidth based on the T<sub>2</sub> times were considerably lower compared to that of the standard  
456 deconvolution fitting (SDF). When applying the same calculations to our samples, the linewidth of the broad signal  
457 at half height is on average 5.2 Hz based on the T<sub>2</sub> times. In contrast, the linewidths acquired from the SDF average  
458 to 256.1 Hz. McLaren et al. (2019) suggested that the broad signal is itself comprised of more than one compound.  
459 Our results are consistent with this view and therefore it is likely that the main cause of the broad signal is a  
460 diversity of P molecules of differing chemical environments within this region, rather than the slow tumbling of  
461 just one macromolecule. Nebbioso and Piccolo (2011) reported that high molecular weight material of organic  
462 matter in soil is an association of smaller organic molecules. We suggest that these associations would still cause  
463 a broad signal in the phosphomonoester region of soil extracts and could be a reason that some organic molecules  
464 containing P are protected from hypobromite oxidation.

465 Since a portion of the broad signal is resistant to hypobromite oxidation, this suggests the organic P is complex  
466 and in the form of polymeric structures. The chemical resistance of the broad signal to hypobromite oxidation may  
467 also indicate a high stability in soil (Jarosch et al., 2015). Annaheim et al. (2015) found that concentrations of the  
468 broad signal remained unchanged between three different organic fertiliser strategies after 62 years of cropping.  
469 In contrast, the organic P compounds annually added with the fertilisers were completely transformed or lost in

470 the slightly acidic topsoil of the field trial. The large proportion of the broad signal in the total organic P pool  
471 demonstrates its importance in the soil P cycle.

472 Unexpectedly, the transverse relaxation times of orthophosphate were shorter than that of the broad signal. This  
473 was similarly the case in an untreated NaOH-EDTA extract of a forest soil with the same origin as the Cambisol  
474 as reported in McLaren et al. (2019). The authors hypothesised that this might be due to the sample matrix (i.e.  
475 high concentration of metals and organic matter). Whilst these factors are likely to affect  $T_2$  times, they do not  
476 appear to be the main cause as the hypobromite oxidised extracts in the current study contained low concentrations  
477 of organic matter and metals as a consequence of the isolation procedure. The fast decay of orthophosphate was  
478 found across all four soil extracts with a diverse array of organic P concentrations and compositions of organic P  
479 in the phosphomonoester region. Therefore, another possible explanation could be a matrix effect or an association  
480 with large organic P compounds causing the broad signal (McLaren et al., 2019). It is known that dynamic  
481 intramolecular processes as ring inversion and intermolecular processes such as binding of small-molecule ligands  
482 to macromolecules can cause a broadening or a doubling of resonances (Claridge, 2016). When the smaller  
483 molecule is bound to the larger molecule, it experiences slower tumbling in the solution and hence a shorter  $T_2$   
484 time. It is possible that a chemical exchange of the orthophosphate with a compound in the matrix or an organic P  
485 molecule could result in the short  $T_2$  time of the orthophosphate peak. We carried out a  $T_2$  experiment on a pure  
486 solution of monopotassium phosphate (described in the Supporting Information), in which the matrix effects  
487 should be considerably reduced compared to the soil extracts. We found that the  $T_2$  time of orthophosphate  
488 (203 ms) in the pure solution was considerably longer than that reported in soil extracts following hypobromite  
489 oxidation.

490 **5 Conclusion**

491 Inositol phosphates are an important pool of organic P in soil, but information on the mechanisms controlling their  
492 flux in soil remain limited due in part to an inability to detect them using solution  $^{31}\text{P}$  NMR spectroscopy. For the  
493 first time, we identified six different lower-order IP in the solution  $^{31}\text{P}$  NMR spectra on soil extracts. Solution  $^{31}\text{P}$   
494 NMR spectra on hypobromite oxidised extracts revealed the presence of up to 70 sharp peaks, which about 50 %  
495 could be identified. Our results indicate that the majority of the sharp peaks in solution  $^{31}\text{P}$  NMR soil spectra were  
496 resistant to hypobromite oxidation, and therefore suggest the presence of diverse IP. Our study highlights the great  
497 diversity and abundance of IP in soils and therefore their importance in terrestrial P cycles. Further research on the  
498 mechanisms and processes involved in the cycling of this wide variety of IP in soil will have implications on our  
499 understanding of organic P turnover as well as plant availability, and possibly help improve fertiliser strategies in  
500 agricultural systems.

501 Furthermore, we provide new insight on the large pool of phosphomonoesters represented by the broad signal, of  
502 which a considerably portion was resistant to hypobromite oxidation. Further research is needed to understand the  
503 chemical composition of the broad signal, and the mechanisms controlling its flux in terrestrial ecosystems.

504 **Data availability**

505 All data presented in this study and the Supplement is also available by request from the corresponding author.

506 **Author contribution**

507 The experimental design was planned by JR, TM, DZ, RV and EF. The experiments were carried out by JR under  
508 supervision of TM, DZ and RV. RV provided the MATLAB code for the standard deconvolution fitting of the  
509 NMR spectra. The data was processed, analysed and interpreted by JR with support from TM, DZ and RV. JR  
510 prepared the manuscript with contributions from all co-authors.

511 **Conflicts of interest**

512 The authors declare that they have no conflict of interest.

513 **Acknowledgements**

514 The authors are grateful to Dr Laurie Paule Schönholzer, Dr Federica Tamburini, Mr Björn Studer, Ms Monika  
515 Macsai, and Dr Charles Bearley for technical support. Furthermore, the authors thank Dr Astrid Oberson, Dr  
516 David Lester, Dr Chiara Pistocchi and Dr Gregor Meyer for providing soil samples. This study would not have  
517 been possible without the IP standards originating from the late Dr Dennis Cosgrove collection and Dr Max Tate  
518 collection, which we highly appreciate. We gratefully acknowledge funding from the Swiss National Science  
519 Foundation [grant number 200021\_169256].

520 **Financial support**

521 This project was funded by the Swiss National Science Foundation, Grant 200021\_169256.

522 **References**

523 Almeida, D. S., Menezes-Blackburn, D., Turner, B. L., Wearing, C., Haygarth, P. M., and Rosolem, C. A.:  
524 *Urochloa ruziziensis* cover crop increases the cycling of soil inositol phosphates, *Biology and Fertility*  
525 of Soils, 54, 935-947, 10.1007/s00374-018-1316-3, 2018.

526 Anderson, G.: Paper chromatography of inositol phosphates, *Nature*, 175, 863-864,  
527 10.1038/175863b0, 1955.

528 Anderson, G., and Arridge, E. Z.: The adsorption of inositol phosphates and glycerophosphate by soil  
529 clays, clay minerals, and hydrated sesquioxides in acid media., *Journal of Soil Science*, 13, 216-224,  
530 10.1111/j.1365-2389.1962.tb00699.x, 1962.

531 Anderson, G., and Malcolm, R. E.: The nature of alkali-soluble soil organic phosphates., *Journal of Soil*  
532 *Science*, 25, 282-297, 10.1111/j.1365-2389.1974.tb01124.x, 1974.

533 Anderson, G., Williams, E. G., and Moir, J. O.: A comparison of the sorption of inorganic  
534 orthophosphate and inositol hexaphosphate by six acid soils, *Journal of Soil Science*, 25, 51-62,  
535 10.1111/j.1365-2389.1974.tb01102.x, 1974.

536 Angyal, S. J.: Chapter VIII - Cyclitols, in: *Comprehensive Biochemistry*, edited by: Florkin, M., and Stotz,  
537 E. H., Elsevier, 297-303, 1963.

538 Annaheim, K. E., Dolette, A. L., Smernik, R. J., Mayer, J., Oberson, A., Frossard, E., and Büinemann, E.  
539 K.: Long-term addition of organic fertilizers has little effect on soil organic phosphorus as characterized  
540 by  $^{31}\text{P}$  NMR spectroscopy and enzyme additions, *Geoderma*, 257-258, 67-77,  
541 <https://doi.org/10.1016/j.geoderma.2015.01.014>, 2015.

542 Baker, R. T.: Changes in the chemical nature of soil organic phosphate during pedogenesis., *Journal of*  
543 *Soil Science*, 27, 504-512, 10.1111/j.1365-2389.1976.tb02020.x, 1976.

544 Borie, F., Zunino, H., and Martínez, L.: Macromolecule - P associations and inositol phosphates in some  
545 chilean volcanic soils of temperate regions, *Communications in Soil Science and Plant Analysis*, 20,  
546 1881-1894, 10.1080/00103628909368190, 1989.

547 Büehler, S., Oberson, A., Sinaj, S., Friesen, D. K., and Frossard, E.: Isotope methods for assessing plant  
548 available phosphorus in acid tropical soils, *European Journal of Soil Science*, 54, 605-616,  
549 10.1046/j.1365-2389.2003.00542.x, 2003.

550 Büinemann, E. K., Smernik, R. J., Marschner, P., and McNeill, A. M.: Microbial synthesis of organic and  
551 condensed forms of phosphorus in acid and calcareous soils, *Soil Biology and Biochemistry*, 40, 932-  
552 946, <https://doi.org/10.1016/j.soilbio.2007.11.012>, 2008.

553 Büinemann, E. K., Augstburger, S., and Frossard, E.: Dominance of either physicochemical or biological  
554 phosphorus cycling processes in temperate forest soils of contrasting phosphate availability, *Soil*  
555 *Biology and Biochemistry*, 101, 85-95, <https://doi.org/10.1016/j.soilbio.2016.07.005>, 2016.

556 Cade-Menun, B., and Liu, C. W.: Solution phosphorus-31 nuclear magnetic resonance spectroscopy of  
557 soils from 2005 to 2013: a review of sample preparation and experimental parameters, *Soil Science*  
558 *Society of America Journal*, 78, 19-37, 10.2136/sssaj2013.05.0187dgs, 2014.

559 Cade-Menun, B. J., and Preston, C. M.: A comparison of soil extraction procedures for  $^{31}\text{P}$  NMR  
560 spectroscopy, *Soil Science*, 161, 1996.

561 Cade-Menun, B. J., Liu, C. W., Nunlist, R., and McColl, J. G.: Soil and litter phosphorus-31 nuclear  
562 magnetic resonance spectroscopy, *Journal of Environmental Quality*, 31, 457-465,  
563 10.2134/jeq2002.4570, 2002.

564 Cade-Menun, B. J.: Improved peak identification in  $^{31}\text{P}$ -NMR spectra of environmental samples with a  
565 standardized method and peak library, *Geoderma*, 257-258, 102-114,  
566 <https://doi.org/10.1016/j.geoderma.2014.12.016>, 2015.

567 Celi, L., and Barberis, E.: Abiotic reactions of inositol phosphates in soil, in: *Inositol phosphates: linking*  
568 *agriculture and the environment*, edited by: Turner, B. L., Richardson, A. E., and Mullaney, E. J., CABI,  
569 Wallingford, 207-220, 2007.

570 Chung, S.-K., Kwon, Y.-U., Chang, Y.-T., Sohn, K.-H., Shin, J.-H., Park, K.-H., Hong, B.-J., and Chung, I.-H.:  
571 Synthesis of all possible regioisomers of *scyllo*-Inositol phosphate, *Bioorganic & Medicinal Chemistry*,  
572 7, 2577-2589, [https://doi.org/10.1016/S0968-0896\(99\)00183-2](https://doi.org/10.1016/S0968-0896(99)00183-2), 1999.

573 Claridge, T. D. W.: Chapter 2 - Introducing High-Resolution NMR, in: High-Resolution NMR techniques  
574 in organic chemistry, 3 ed., edited by: Claridge, T. D. W., Elsevier, Boston, 11-59, 2016.

575 Cosgrove, D.: The chemical nature of soil organic phosphorus. I. Inositol phosphates, *Soil Research*, 1,  
576 203-214, <https://doi.org/10.1071/SR9630203>, 1963.

577 Cosgrove, D. J., and Irving, G. C. J.: Inositol phosphates : their chemistry, biochemistry and physiology,  
578 Studies in organic chemistr, Amsterdam : Elsevier, 1980.

579 Doolette, A. L., Smernik, R. J., and Dougherty, W. J.: Spiking improved solution phosphorus-31 nuclear  
580 magnetic resonance identification of soil phosphorus compounds, *Soil Science Society of America  
581 Journal*, 73, 919-927, 10.2136/sssaj2008.0192, 2009.

582 Doolette, A. L., Smernik, R. J., and Dougherty, W. J.: A quantitative assessment of phosphorus forms in  
583 some Australian soils, *Soil Research*, 49, 152-165, <https://doi.org/10.1071/SR10092>, 2011a.

584 Doolette, A. L., Smernik, R. J., and Dougherty, W. J.: Overestimation of the importance of phytate in  
585 NaOH-EDTA soil extracts as assessed by <sup>31</sup>P NMR analyses, *Organic Geochemistry*, 42, 955-964,  
586 <https://doi.org/10.1016/j.orggeochem.2011.04.004>, 2011b.

587 Doolette, A. L., and Smernik, R. J.: Phosphorus speciation of dormant grapevine (*Vitis vinifera* L.) canes  
588 in the Barossa Valley, South Australia, *Australian Journal of Grape and Wine Research*, 22, 462-468,  
589 10.1111/ajgw.12234, 2016.

590 Doolette, A. L., and Smernik, R. J.: Facile decomposition of phytate in the solid-state: kinetics and  
591 decomposition pathways, *Phosphorus, Sulfur, and Silicon and the Related Elements*, 193, 192-199,  
592 10.1080/10426507.2017.1416614, 2018.

593 Dougherty, W. J., Smernik, R. J., and Chittleborough, D. J.: Application of spin counting to the solid-  
594 state <sup>31</sup>P NMR analysis of pasture soils with varying phosphorus content, *Soil Science Society of  
595 America Journal*, 69, 2058-2070, 10.2136/sssaj2005.0017, 2005.

596 Dougherty, W. J., Smernik, R. J., Bünemann, E. K., and Chittleborough, D. J.: On the use of hydrofluoric  
597 acid pretreatment of soils for phosphorus-31 nuclear magnetic resonance analyses, *Soil Science  
598 Society of America Journal*, 71, 1111-1118, 10.2136/sssaj2006.0300, 2007.

599 Dyer, W. J., and Wrenshall, C. L.: Organic phosphorus in soils: III. The decomposition of some organic  
600 phosphorus compounds in soil cultures, *Soil Sci.*, 51, 323, 1941.

601 FAO, and Group, I. W.: World reference base for soil resources 2014, *World soil resources reports*,  
602 Food and Agriculture Organization of the United Nations FAO, Rome, 2014.

603 Fatiadi, A. J.: Bromine oxidation of inositol for preparation of inosose phenylhydrazones and  
604 phenylosazones, *Carbohydrate Research*, 8, 135-147, [https://doi.org/10.1016/S0008-6215\(00\)80149-4](https://doi.org/10.1016/S0008-6215(00)80149-4), 1968.

605 Goring, C. A. I., and Bartholomew, W. V.: Microbial products and soil organic matter: III. Adsorption of  
606 carbohydrate phosphates by clays, *Soil Science Society of America Journal*, 15, 189-194,  
607 10.2136/sssaj1951.036159950015000C0043x, 1951.

608 Halstead, R. L., and Anderson, G.: Chromatographic fractionation of organic phosphates from alkali,  
609 acid, and aqueous acetylacetone extracts of soils, *Canadian Journal of Soil Science*, 50, 111-119,  
610 10.4141/cjss70-018, 1970.

611 Hochberg, Y., and Tamhane, A. C.: Multiple comparison procedures, Wiley series in probability and  
612 mathematical statistics. Applied probability and statistics, Wiley New York, 1987.

613 Irvine, R. F., and Schell, M. J.: Back in the water: the return of the inositol phosphates, *Nature Reviews  
614 Molecular Cell Biology*, 2, 327, 10.1038/35073015, 2001.

615 Irving, G. C. J., and Cosgrove, D. J.: The use of hypobromite oxidation to evaluate two current methods  
616 for the estimation of inositol polyphosphates in alkaline extracts of soils, *Communications in Soil  
617 Science and Plant Analysis*, 12, 495-509, 10.1080/00103628109367169, 1981.

618 Irving, G. C. J., and Cosgrove, D. J.: The use of gas - liquid chromatography to determine the  
619 proportions of inositol isomers present as pentakis - and hexakisphosphates in alkaline extracts of  
620 soils, *Communications in Soil Science and Plant Analysis*, 13, 957-967, 10.1080/00103628209367324,  
621 1982.

622 Jarosch, K. A., Doolette, A. L., Smernik, R. J., Tamburini, F., Frossard, E., and Bünemann, E. K.:  
623 Characterisation of soil organic phosphorus in NaOH-EDTA extracts: a comparison of <sup>31</sup>P NMR

625 spectroscopy and enzyme addition assays, *Soil Biology and Biochemistry*, 91, 298-309,  
626 <https://doi.org/10.1016/j.soilbio.2015.09.010>, 2015.

627 L'Annunziata, M. F.: The origin and transformations of the soil inositol phosphate isomers, *Soil Science*  
628 *Society of America Journal*, 39, 377-379, 10.2136/sssaj1975.03615995003900020041x, 1975.

629 Lang, F., Krüger, J., Amelung, W., Willbold, S., Frossard, E., Büinemann, E. K., Bauhus, J., Nitschke, R.,  
630 Kandeler, E., Marhan, S., Schulz, S., Bergkemper, F., Schloter, M., Luster, J., Guggisberg, F., Kaiser, K.,  
631 Mikutta, R., Guggenberger, G., Polle, A., Pena, R., Prietzl, J., Rodionov, A., Talkner, U., Meesenburg,  
632 H., von Wilpert, K., Hölscher, A., Dietrich, H. P., and Chmara, I.: Soil phosphorus supply controls P  
633 nutrition strategies of beech forest ecosystems in Central Europe, *Biogeochemistry*, 136, 5-29,  
634 10.1007/s10533-017-0375-0, 2017.

635 Leytem, A. B., Turner, B. L., and Thacker, P. A.: Phosphorus composition of manure from swine fed low-  
636 phyteate grains, *Journal of Environmental Quality*, 33, 2380-2383, 10.2134/jeq2004.2380, 2004.

637 Leytem, A. B., and Maguire, R. O.: Environmental implications of inositol phosphates in animal  
638 manures, in: *Inositol phosphates: linking agriculture and the environment*, edited by: Turner, B. L.,  
639 Richardson, A. E., and Mullaney, E. J., CABI, Wallingford, 150-168, 2007.

640 Li, M., Cozzolino, V., Mazzei, P., Drosos, M., Monda, H., Hu, Z., and Piccolo, A.: Effects of microbial  
641 bioeffectors and P amendments on P forms in a maize cropped soil as evaluated by  $^{31}\text{P}$ -NMR  
642 spectroscopy, *Plant and Soil*, 427, 87-104, 10.1007/s11104-017-3405-8, 2018.

643 Makarov, M. I., Malysheva, T. I., Haumaier, L., Alt, H. G., and Zech, W.: The forms of phosphorus in  
644 humic and fulvic acids of a toposequence of alpine soils in the northern Caucasus, *Geoderma*, 80, 61-  
645 73, [https://doi.org/10.1016/S0016-7061\(97\)00049-9](https://doi.org/10.1016/S0016-7061(97)00049-9), 1997.

646 McDowell, R. W., and Stewart, I.: The phosphorus composition of contrasting soils in pastoral, native  
647 and forest management in Otago, New Zealand: Sequential extraction and  $^{31}\text{P}$  NMR, *Geoderma*, 130,  
648 176-189, <https://doi.org/10.1016/j.geoderma.2005.01.020>, 2006.

649 McDowell, R. W., Cade-Menun, B., and Stewart, I.: Organic phosphorus speciation and pedogenesis:  
650 analysis by solution  $^{31}\text{P}$  nuclear magnetic resonance spectroscopy, *European Journal of Soil Science*,  
651 58, 1348-1357, 10.1111/j.1365-2389.2007.00933.x, 2007.

652 McKercher, R. B., and Anderson, G.: Characterization of the inositol penta- and hexaphosphate  
653 fractions of a number of Canadian and Scottish soils, *Journal of Soil Science*, 19, 302-310,  
654 10.1111/j.1365-2389.1968.tb01542.x, 1968a.

655 McKercher, R. B., and Anderson, G.: Content of inositol penta- and hexaphosphates in some Canadian  
656 soils, *Journal of Soil Science*, 19, 47-55, 10.1111/j.1365-2389.1968.tb01519.x, 1968b.

657 McKercher, R. B., and Anderson, G.: Organic phosphate sorption by neutral and basic soils,  
658 *Communications in Soil Science and Plant Analysis*, 20, 723-732, 10.1080/00103628909368112, 1989.

659 McLaren, T. I., Smernik, R. J., Guppy, C. N., Bell, M. J., and Tighe, M. K.: The organic P composition of  
660 vertisols as determined by  $^{31}\text{P}$  NMR spectroscopy, *Soil Science Society of America Journal*, 78, 1893-  
661 1902, 10.2136/sssaj2014.04.0139, 2014.

662 McLaren, T. I., Simpson, R. J., McLaughlin, M. J., Smernik, R. J., McBeath, T. M., Guppy, C. N., and  
663 Richardson, A. E.: An assessment of various measures of soil phosphorus and the net accumulation of  
664 phosphorus in fertilized soils under pasture, *Journal of Plant Nutrition and Soil Science*, 178, 543-554,  
665 10.1002/jpln.201400657, 2015a.

666 McLaren, T. I., Smernik, R. J., McLaughlin, M. J., McBeath, T. M., Kirby, J. K., Simpson, R. J., Guppy, C.  
667 N., Doolittle, A. L., and Richardson, A. E.: Complex forms of soil organic phosphorus—A major  
668 component of soil phosphorus, *Environmental Science & Technology*, 49, 13238-13245,  
669 10.1021/acs.est.5b02948, 2015b.

670 McLaren, T. I., Verel, R., and Frossard, E.: The structural composition of soil phosphomonoesters as  
671 determined by solution  $^{31}\text{P}$  NMR spectroscopy and transverse relaxation ( $T_2$ ) experiments, *Geoderma*,  
672 345, 31-37, <https://doi.org/10.1016/j.geoderma.2019.03.015>, 2019.

673 Meiboom, S., and Gill, D.: Modified spin - echo method for measuring nuclear relaxation times, *Review*  
674 *of Scientific Instruments*, 29, 688-691, 10.1063/1.1716296, 1958.

675 Milliken, G. A., and Johnson, D. E.: *Analysis of messy data. Volume 1: designed experiments*, 2nd ed.  
676 ed., Boca Raton, Fla : CRC Press, 2009.

677 Newman, R. H., and Tate, K. R.: Soil phosphorus characterisation by  $^{31}\text{P}$  nuclear magnetic resonance, Communications in Soil Science and Plant Analysis, 11, 835-842, 10.1080/00103628009367083, 1980.

679 Ognalaga, M., Frossard, E., and Thomas, F.: Glucose-1-phosphate and *myo*-inositol hexaphosphate adsorption mechanisms on goethite, Soil Science Society of America Journal, 58, 332-337, 10.2136/sssaj1994.03615995005800020011x, 1994.

682 Ohno, T., and Zibilske, L. M.: Determination of low concentrations of phosphorus in soil extracts using malachite green, Soil Science Society of America Journal, 55, 892-895, 10.2136/sssaj1991.03615995005500030046x, 1991.

685 Reusser, J. E., Verel, R., Frossard, E., and McLaren, T. I.: Quantitative measures of *myo*-IP<sub>6</sub> in soil using solution  $^{31}\text{P}$  NMR spectroscopy and spectral deconvolution fitting including a broad signal, Environmental Science: Processes & Impacts, 10.1039/C9EM00485H, 2020.

688 Riley, A. M., Trusselle, M., Kuad, P., Borkovec, M., Cho, J., Choi, J. H., Qian, X., Shears, S. B., Spiess, B., and Potter, B. V. L.: *scyllo* - Inositol pentakisphosphate as an analogue of *myo* - inositol 1,3,4,5,6 - pentakisphosphate: Chemical synthesis, physicochemistry and biological applications, ChemBioChem, 7, 1114-1122, 10.1002/cbic.200600037, 2006.

692 Sharma, V. K.: Oxidation of amino acids, peptides, and proteins : kinetics and mechanism, Wiley series of reactive intermediates in chemistry and biology, Hoboken : Wiley, 2013.

694 Smith, D. H., and Clark, F. E.: Anion-exchange chromatography of inositol phosphates from soil, Soil Science, 72, 353-360, 1951.

696 Spain, A. V., Tibbett, M., Ridd, M., and McLaren, T. I.: Phosphorus dynamics in a tropical forest soil restored after strip mining, Plant and Soil, 427, 105-123, 10.1007/s11104-018-3668-8, 2018.

698 Stephens, L. R., and Irvine, R. F.: Stepwise phosphorylation of *myo*-inositol leading to *myo*-inositol hexakisphosphate in *Dictyostelium*, Nature, 346, 580-583, 10.1038/346580a0, 1990.

700 Strickland, K. P.: The chemistry of phospholipids, Second, completely revised and enlarged edition. ed., Form and Function of Phospholipids, edited by: Ansell, G. B., Hawthorne, J. N., and Dawson, R. M. C., Elsevier Scientific Publ. Company, 1973.

703 Sun, M., Alikhani, J., Massoudieh, A., Greiner, R., and Jaisi, D. P.: Phytate degradation by different phosphohydrolase enzymes: contrasting kinetics, decay rates, pathways, and isotope effects, Soil Science Society of America Journal, 81, 61-75, 10.2136/sssaj2016.07.0219, 2017.

706 Sun, M., and Jaisi, D. P.: Distribution of inositol phosphates in animal feed grains and excreta: distinctions among isomers and phosphate oxygen isotope compositions, Plant and Soil, 430, 291-305, 10.1007/s11104-018-3723-5, 2018.

709 Suzumura, M., and Kamatani, A.: Isolation and determination of inositol hexaphosphate in sediments from Tokyo Bay, Geochimica et Cosmochimica Acta, 57, 2197-2202, [https://doi.org/10.1016/0016-7037\(93\)90561-A](https://doi.org/10.1016/0016-7037(93)90561-A), 1993.

712 Turner, B. L., Papházy, M. J., Haygarth, P. M., and McKelvie, I. D.: Inositol phosphates in the environment, Philosophical Transactions of the Royal Society of London. Series B: Biological Sciences, 357, 449, 2002.

715 Turner, B. L., and Richardson, A. E.: Identification of *scyllo*-inositol phosphates in soil by solution phosphorus-31 nuclear magnetic resonance spectroscopy, Soil Science Society of America Journal, 68, 802-808, 10.2136/sssaj2004.8020, 2004.

718 Turner, B. L.: Inositol phosphates in soil: Amounts, forms and significance of the phosphorylated inositol stereoisomers., in: Inositol phosphates: Linking agriculture and the environment., edited by: Turner, B. L., Richardson, A. E., and Mullaney, E. J., CAB International, Wallingford, Oxfordshire, UK, 186-206, 2007.

722 Turner, B. L., Condron, L. M., Richardson, S. J., Peltzer, D. A., and Allison, V. J.: Soil organic phosphorus transformations during pedogenesis, Ecosystems, 10, 1166-1181, 10.1007/s10021-007-9086-z, 2007a.

724 Turner, B. L., Richardson, A. E., and Mullaney, E. J.: Inositol phosphates: linking agriculture and the environment, CABI, Wallingford, xi + 288 pp. pp., 2007b.

726 Turner, B. L.: Soil organic phosphorus in tropical forests: an assessment of the NaOH-EDTA extraction procedure for quantitative analysis by solution  $^{31}\text{P}$  NMR spectroscopy, European Journal of Soil Science, 59, 453-466, 10.1111/j.1365-2389.2007.00994.x, 2008.

729 Turner, B. L., Cheesman, A. W., Godage, H. Y., Riley, A. M., and Potter, B. V.: Determination of *neo*- and  
730 D-*chiro*-inositol hexakisphosphate in soils by solution  $^{31}\text{P}$  NMR spectroscopy, *Environ Sci Technol*, 46,  
731 4994-5002, 10.1021/es204446z, 2012.

732 Turner, B. L., Wells, A., and Condron, L. M.: Soil organic phosphorus transformations along a coastal  
733 dune chronosequence under New Zealand temperate rain forest, *Biogeochemistry*, 121, 595-611,  
734 10.1007/s10533-014-0025-8, 2014.

735 Turner, B. L.: Isolation of inositol hexakisphosphate from soils by alkaline extraction and hypobromite  
736 oxidation, in: *Inositol Phosphates: Methods and Protocols*, edited by: Miller, G. J., Springer US, New  
737 York, NY, 39-46, 2020.

738 Vestergren, J., Vincent, A. G., Jansson, M., Persson, P., Ilstedt, U., Gröbner, G., Giesler, R., and  
739 Schleucher, J.: High-resolution characterization of organic phosphorus in soil extracts using 2D  $^1\text{H}$ - $^{31}\text{P}$   
740 NMR correlation spectroscopy, *Environmental Science & Technology*, 46, 3950-3956,  
741 10.1021/es204016h, 2012.

742 Vincent, A. G., Vestergren, J., Gröbner, G., Persson, P., Schleucher, J., and Giesler, R.: Soil organic  
743 phosphorus transformations in a boreal forest chronosequence, *Plant and Soil*, 367, 149-162,  
744 10.1007/s11104-013-1731-z, 2013.

745 Vold, R. L., Waugh, J. S., Klein, M. P., and Phelps, D. E.: Measurement of spin relaxation in complex  
746 systems, *The Journal of Chemical Physics*, 48, 3831-3832, 10.1063/1.1669699, 1968.

747 Volkmann, C. J., Chateauneuf, G. M., Pradhan, J., Bauman, A. T., Brown, R. E., and Murthy, P. P. N.:  
748 Conformational flexibility of inositol phosphates: influence of structural characteristics, *Tetrahedron  
749 Letters*, 43, 4853-4856, [https://doi.org/10.1016/S0040-4039\(02\)00875-4](https://doi.org/10.1016/S0040-4039(02)00875-4), 2002.

750

751

**Table 1. General characteristics of soil samples used in this study.**

Soil type	-	Ferralsol	Vertisol	Cambisol	Gleysol
Country	-	Colombia	Australia	Germany	Switzerland
Coordinates sampling site	-	4°30' N / 71°19' W	27°52' S / 151°37' E	50°21' N / 9°55' E	47°05' N / 8°06' E
Elevation	m ASL	150	402	800	612
Sampling depth	cm	0-20	0-15	0-7	0-10
Year of sampling	year	1997	2017	2014	2017
Land use	-	Pasture	Arable field	Forest	Pasture
C <sub>tot</sub>	g C/kg <sub>soil</sub>	26.7	23.9	90.3	148.3
N <sub>tot</sub>	g N/kg <sub>soil</sub>	1.7	1.9	6.6	10.9
pH in H <sub>2</sub> O	-	3.6	6.1	3.6	5.0

**Table 2. Standard solutions used for the spiking experiment of the hypobromite oxidised soil extracts. All standards were dissolved in 0.25 M NaOH and 0.05 M Na<sub>2</sub>EDTA.**

Standard	Product number	Company/origin	Concentration of standard in NaOH-EDTA (mg/mL)
<i>myo</i> -IP <sub>6</sub>	P5681	Merck (Sigma-Aldrich)	8.10
L- <i>chiro</i> -IP <sub>6</sub>	Collection of Dr Max Tate		2.39
D- <i>chiro</i> -IP <sub>6</sub>	CAY-9002341	Cayman Chemical	2.00
<i>neo</i> -IP <sub>6</sub>	Collection of Dr Dennis Cosgrove, made up in 15 mM HCl		4.62
D- <i>myo</i> -(1,2,4,5,6)-IP <sub>5</sub>	CAY-10008452-1	Cayman Chemical	2.00
<i>myo</i> -(1,2,3,4,6)-IP <sub>5</sub>	93987	Merck (Sigma-Aldrich)	2.00
D- <i>myo</i> -(1,3,4,5,6)-IP <sub>5</sub>	CAY-10009851-1	Cayman Chemical	2.00
D- <i>myo</i> -(1,2,3,5,6)-IP <sub>5</sub>	CAY-10008453-1	Cayman Chemical	2.00
<i>scyllo</i> -IP <sub>5</sub>	Collection of Dr Dennis Cosgrove		2.64
L- <i>chiro</i> -IP <sub>5</sub>	Collection of Dr Dennis Cosgrove		2.24
<i>neo</i> -IP <sub>5</sub>	Collection of Dr Dennis Cosgrove		2.45
<i>myo</i> -IP <sub>4</sub>	Collection of Dr Dennis Cosgrove		2.76
<i>scyllo</i> -IP <sub>4</sub>	Collection of Dr Dennis Cosgrove		2.41
<i>neo</i> -IP <sub>4</sub>	Collection of Dr Dennis Cosgrove		2.33

757 **Table 3. Concentrations of total P as measured by XRF and 0.25 M NaOH + 0.05 M EDTA extractable P before and**  
 758 **after hypobromite oxidation of soil extracts. Concentrations of total P in NaOH-EDTA extracts were determined by**  
 759 **ICP-OES, whereas that of molybdate reactive P (MRP) was determined by the malachite green method of Ohno and**  
 760 **Zibilske (1991). Concentrations of molybdate unreactive P (MUP) were calculated as the difference between total P and**  
 761 **MRP.**

Measure		Ferralsol	Vertisol	Cambisol	Gleysol
<b>XRF</b>	$P_{tot}$ (mg P/kg <sub>soil</sub> )	320	1726	3841	2913
<b>NaOH-EDTA extractable P (untreated)</b>	$P_{tot}$ (mg P/kg <sub>soil</sub> )	160	484	1850	1490
	MRP (mg P/kg <sub>soil</sub> )	67	351	525	610
	MUP (P <sub>org</sub> ) (mg P/kg <sub>soil</sub> )	93	133	1326	880
<b>NaOH-EDTA extractable P (hypobromite oxidised)</b>	$P_{tot}$ (mg P/kg <sub>soil</sub> )	77	158	580	578
	MRP (mg P/kg <sub>soil</sub> )	32	111	283	231
	MUP (P <sub>org</sub> ) (mg P/kg <sub>soil</sub> )	45	47	297	348

762

763  
764 **Table 4. Concentrations (mg P/kg<sub>soil</sub>) of P compounds in solution <sup>31</sup>P NMR spectra of 0.25 M NaOH + 0.05 M EDTA**  
765 **soil extracts (Ferralsol, Vertisol, Cambisol and Gleysol) before and after hypobromite oxidation (HO). Quantification**  
766 **was based on spectral integration and deconvolution fitting. The proportion of P detected in hypobromite oxidised**  
**extracts compared to that in untreated extracts is provided in brackets.**

Phosphorus class		Ferralsol	Vertisol	Cambisol	Gleysol
<b>Phosphonates</b>	before HO	1.0	2.6	14.5	-
	after HO	-	-	3.0 (21)	0.2
<b>Orthophosphate</b>	before HO	54.8	221.4	434.3	368.3
	after HO	32.0 (58)	116.6 (53)	329.3 (76)	243.4 (66)
<b>Phosphomonoester</b>	before HO	36.3	39.1	501.1	399.2
	after HO	12.7 (35)	24.2 (62)	210.3 (42)	292.1 (73)
<b>Broad peak in phosphomonoester region</b>	before HO	21.6	30.9	305.8	216.7
	after HO	8.3 (39)	19.3 (63)	99.2 (32)	108.4 (50)
<b>Phosphodiester</b>	before HO	5.1	-	28.2	26.9
	after HO	-	-	-	2.0 (8)
<b>Pyrophosphate</b>	before HO	1.9	1.8	12.9	23.9
	after HO	-	-	-	-

768  
769  
770  
771  
772  
773 **Table 5. Concentrations of identified inositol phosphates (IP) in hypobromite oxidised 0.25 M NaOH + 0.05 M EDTA**  
soil extracts (Ferralsol, Vertisol, Cambisol and Gleysol). Concentrations were calculated from solution  $^{31}\text{P}$  NMR spectra  
using spectral deconvolution fitting including an underlying broad signal. When no concentration is given, the IP  
compound was not detected in the respective soil extract. Chemical shift positions are based on the NMR spectrum of  
the Cambisol extract (Fig. SI8 in the Supporting Information). Peak positions varied up to +0.018 ppm (Gleysol).  
Conformation equatorial (eq) and axial (ax) according to Turner et al. (2012).

Phosphorus compound	Chemical shift $\delta$ ppm	Concentrations (mg P/kg <sub>soil</sub> )			
		Ferralsol	Vertisol	Cambisol	Gleysol
<i>myo</i> -IP <sub>6</sub>	4.97, 4.06, 3.70, 3.57	1.1	0.6	26.3	85.0
<i>scyllo</i> -IP <sub>6</sub>	3.20	0.4	0.3	15.6	41.1
<i>neo</i> -IP <sub>6</sub> 4-eq/2-ax	5.86, 3.75	-	-	1.4	8.8
<i>neo</i> -IP <sub>6</sub> 2-eq/4-ax	4.36, 4.11	-	-	4.0	1.3
D- <i>chiro</i> -IP <sub>6</sub> 2-eq/4-ax	5.66, 4.25, 3.83	-	-	9.4	8.6
<i>myo</i> -(1,2,4,5,6)-IP <sub>5</sub>	4.42, 3.97, 3.72, 3.36, 3.25	-	-	7.0	4.1
<i>myo</i> -(1,3,4,5,6)-IP <sub>5</sub>	4.12, 3.60, 3.23	-	-	2.8	1.3
<i>scyllo</i> -IP <sub>5</sub>	3.81, 3.31, 3.05	0.7	0.5	10.8	6.1
<i>neo</i> -IP <sub>5</sub>	4.64, 4.27, 4.01, 3.87, 3.13	-	-	3.3	2.1
<i>chiro</i> -IP <sub>5</sub>	4.61, 3.39	-	-	0.9	-
<i>scyllo</i> -(1,2,3,4)-IP <sub>4</sub>	4.12, 3.25	0.8	-	4.3	1.0
<b>Total IP</b>		3.0	1.4	85.9	159.3

774

775  
776  
777

**Table 6. Transversal relaxation times ( $T_2$ ) of various P species in the orthophosphate and phosphomonoester regions as determined by solution  $^{31}\text{P}$  nuclear magnetic resonance (NMR) spectroscopy and a Carr-Purcell- Meiboom-Gill (CPMG) pulse sequence on hypobromite oxidised soil extracts.**

Phosphorus compound	$T_2$ [ms]				778
	Ferralsol	Vertisol	Cambisol	Gleysol	
<i>myo</i> -IP <sub>6</sub>	163	140	139	121	
<i>scyllo</i> -IP <sub>6</sub>	250	155	154	144	
<i>neo</i> -IP <sub>6</sub>	-	-	203	102	
<i>D-chiro</i> -IP <sub>6</sub>	-	-	108	132	
<b>orthophosphate</b>	14	9	17	6	
<b>broad peak</b>	44	69	89	62	